

# Determination of light absorption, scattering and anisotropy factor of a highly scattering medium using backscattered circularly polarized light

M. Xu<sup>a</sup>, M. Alrubaiee<sup>b</sup>, S. K. Gayen<sup>b</sup> and R. R. Alfano<sup>b</sup>

<sup>a</sup>Department of Physics, Fairfield University, Connecticut, CT 06824

<sup>b</sup>Institute for Ultrafast Spectroscopy and Lasers and Department of Physics,  
The City College and Graduate Center of City University of New York, New York, NY 10031  
Email: mxu@mail.fairfield.edu

## ABSTRACT

The absorption coefficient, the scattering coefficient and the anisotropy factor of a highly scattering medium are determined using the diffuse reflectance of an obliquely incident beam of circularly polarized light. This approach determines both the anisotropy factor and the cutoff size parameter for the fractal continuous scattering medium such as biological tissue and tissue phantoms from depolarization of the backscattered light.

**Keywords:** absorption, scattering, anisotropy factor, backscattering, depolarization, circular polarization, tissue, turbid medium

## 1. INTRODUCTION

The estimation of the optical properties (absorption coefficient  $\mu_a$  and scattering coefficient  $\mu_s$ ) and the anisotropy factor ( $g$ ) of a turbid medium is an important problem in atmospheric, biomedical and hydrologic optics. Light diffuses in a highly scattering medium, whose behavior essentially depends on the reduced scattering coefficient  $\mu'_s = \mu_s(1 - g)$ . The diffusion of light remains almost the same when varying  $\mu_s$  and  $g$  yet keeping  $\mu'_s$  unchanged. This explains why  $\mu_a$  and  $\mu'_s$ , instead of  $\mu_a$ ,  $\mu_s$  and  $g$ , are commonly used in optical imaging. Light absorption and scattering coefficients depend on the optical properties of constituent particles and their concentration. The  $g$ -factor measures how much forward peaked is the angular distribution of light when it is scattered once by a particle in the medium, and is independent of the concentration of the scatterers. The value of the  $g$ -factor correlates strongly with the size of the scatterer. Determination of the  $g$ -factor then provides a direct probe of the size of scatterer, which constitutes one useful fingerprint in discriminating normal and diseased tissues.<sup>1, 2</sup>

One way to estimate the  $g$ -factor is to use an iterative method that consists of repeatedly solving the corresponding direct radiative transfer problem by, for example, Monte Carlo simulations, with updated optical properties until the irradiance matches the measured values.<sup>3</sup> Explicit analytical equations have also been developed (analytic inverse radiative transfer method) for determining the optical properties in the simplest problems.<sup>4</sup> In both approaches, the type of the phase function of light scattering by the medium is usually assumed known and the Henyey-Greenstein phase function<sup>5</sup> has been commonly used.

In this paper, we report on a scheme of detecting light absorption coefficient, scattering coefficient and the  $g$ -factor simultaneously from measurement of the circularly polarized backscattered light at different positions along a line. Light is obliquely incident on the surface of the medium with an incidence angle  $\sim 70$  degree. Both co-polarized and cross-polarized backscattered light are measured. The difference of the backscattered co-polarized and cross-polarized light intensities is used to find the  $g$ -factor of the medium. Experimental demonstrations of this approach to obtain the three parameters (absorption coefficient, scattering coefficient and the  $g$ -factor) of tissue phantoms are presented.

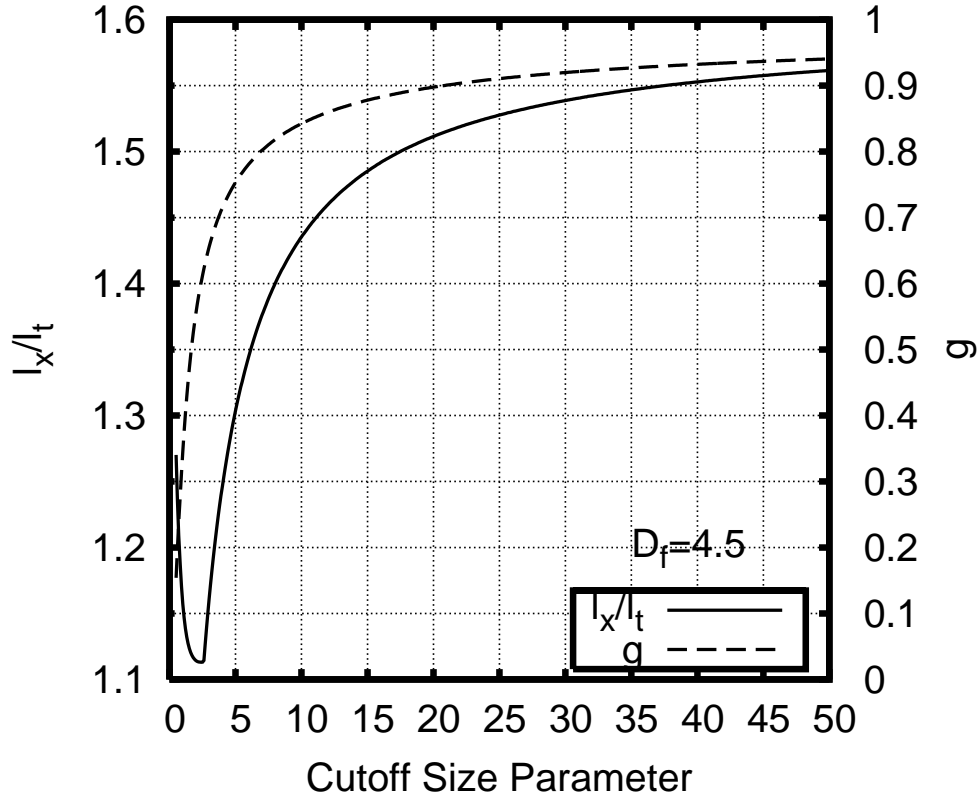


**Figure 1.** The ratio of the uncoiling length over the transport mean free path  $l_x/l_t$  and the anisotropy factor  $g$  of soft tissue of a fractal dimension 4.5 and of varying cutoff size parameter  $X = 2\pi n l_{\max}/\lambda$ .

## 2. THEORETICAL FORMALISM AND EXPERIMENTAL METHOD

Light propagation in a turbid medium can be described by radiative transfer theory. Diffusion approximation to radiative transfer theory is a valid model for light propagation if the medium is highly scattering and optically thick. For a polarized incident beam, light propagation in the medium accompanies its depolarization. The characteristic lengths governing light depolarization in turbid media have been obtained earlier.<sup>6,7</sup> The depolarization of circularly polarized light is found to be determined by the uncoiling length  $l_x$ , the distance over which the degree of circular polarization of the beam drops by  $1/e$ . The uncoiling length for a turbid medium is given by<sup>7</sup>

$$l_x \equiv \mu_s^{-1} / \ln \frac{1}{\lambda_x} \quad (1)$$

where  $\lambda_x = \max(\Lambda_0, \Lambda_1)$ ,  $\Lambda_0 = \frac{1}{2\gamma} \int_{-1}^1 \Re[S_1^* S_2] d\mu$ ,  $\Lambda_1 = \frac{1}{2\gamma} \int_{-1}^1 \Re[S_1^* S_2] \mu d\mu$ ,  $\gamma = \frac{1}{4} \int_{-1}^1 (|S_1|^2 + |S_2|^2) d\mu$ ,  $\mu \equiv \cos \theta$ , and  $S_{1,2}(\theta)$  is the amplitude scattering function with  $\theta$  the scattering angle.<sup>8</sup>

Light scattering by biological tissue and cells can be described by the fractal continuous random medium model.<sup>1,2</sup> In this model, tissue light scattering is determined by two morphological parameters: the fractal dimension  $D_f$  and the cutoff correlation length  $l_{\max}$ . The parameter  $D_f$  reveals the weight of small vs large scattering centers in the sample and  $l_{\max}$  measures the maximum size of scattering centers. Light depolarization characteristic lengths, including the uncoiling length  $l_x$ , in biological tissue and tissue phantoms have been investigated.<sup>9</sup> Fig. (1) displays the ratio  $l_x/l_t$  and the  $g$ -factor versus the cutoff size parameter  $X = 2\pi n l_{\max}/\lambda$  for a fractal continuous random medium with  $D_f = 4.5$  where  $n$  is the refractive index of the medium and  $\lambda$  is the wavelength of the incident beam in vacuum. This figure suggests that the anisotropy factor  $g$  (and  $l_{\max}$ ) can be determined if the fractal dimension  $D_f$  and the uncoiling length  $l_x$  can be found in addition to the transport mean free path  $l_t$ .

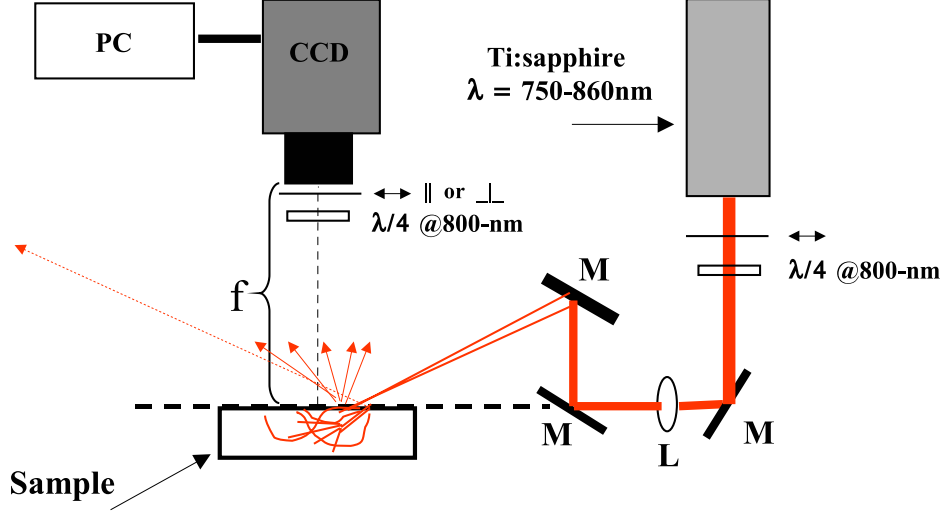


**Figure 2.** Schematic diagram of the experimental setup. M stands for mirror, L lens, and  $f$  is the focal length of the CCD camera. The  $\lambda/4$  wave plates and polarizers are used to generate a circularly polarized beam and to detect co- or cross-polarized light at the wavelength of 800nm.

Our procedure for the determination of  $\mu_a$ ,  $\mu_s$  and  $g$  is as follows. First  $\mu_a$  and  $\mu'_s$  are determined from the diffuse reflectance of the sample for an obliquely incident beam at various wavelengths centering at  $\lambda$ . Second, the fractal dimension  $D_f$  is determined from  $\mu'_s(\lambda) \propto \lambda^{3-D_f}$ . Third, the uncoiling length  $l_x$  is found from the depolarized diffuse reflectance of a circularly polarized incident beam. And finally, the anisotropy factor  $g$  is obtained by the ratio of  $l_x/l_t$  (see Fig. 1). The first two steps can be combined to retrieve  $\mu_a$ ,  $\mu'_s$  and  $D_f$  simultaneously from fitting to the diffuse reflectance data at all wavelengths together assuming the power law for  $\mu'_s(\lambda)$  is strictly satisfied.

For an obliquely incident pencil beam at the origin on the surface  $z = 0$  of the sample and propagating in the direction  $(\sin \alpha, 0, -\cos \alpha)$  where  $\alpha$  is the angle of incidence, the initial ballistic motion of the beam within the medium is in the direction  $(\sin \beta, 0, -\cos \beta)$  where  $n \sin \beta = \sin \alpha$ . The diffuse reflectance at the position  $(x, y, 0)$  on the surface is given by<sup>10</sup>

$$R(x, y) = \frac{l_t \cos \beta}{4\pi\rho_1^3} (1 + \mu_{\text{eff}}\rho_1) \exp(-\mu_{\text{eff}}\rho_1) + \frac{l_t \cos \beta + 2z_e}{4\pi\rho_2^3} (1 + \mu_{\text{eff}}\rho_2) \exp(-\mu_{\text{eff}}\rho_2), \quad (2)$$

where  $\mu_{\text{eff}} = \sqrt{3\mu_a/l_t}$ ,  $\rho_1 = \sqrt{(x - l_t \sin \beta)^2 + y^2 + l_t^2 \cos^2 \beta}$ , and  $\rho_2 = \sqrt{(x - l_t \sin \beta)^2 + y^2 + (2z_e + l_t \cos \beta)^2}$ . The parameter  $z_e$  is the extrapolation length, dependent on the refractive index mismatch at the interface.<sup>11</sup> Eq. (2) is used to fit the measured diffuse reflectance along a line in the  $x$  direction on the surface to obtain  $\mu_a$  and  $l_t$ .

For an incident circularly polarized beam, light depolarization presents one extra channel that light leaves the co-polarized state to the cross-polarized state. Denote the co-polarized and cross-polarized backscattered light intensity for an incident circularly polarized light as  $I_{\pm}$ , respectively. The depolarized diffuse reflectance is proportional to  $\Delta I = I_+ - I_-$  and can be modelled by the same expression (2) with the only modification of  $\mu_a \rightarrow \mu'_a = \mu_a + l_x^{-1}$ . The same technique hence can be used to fit for  $l_x$  in the region far away from the incidence point where the diffusion model is valid.

The experimental setup is shown in Fig. 2. The light source is a Ti:sapphire laser (Spectra-Physics Tsunami) tunable over the 750–860nm spectral range. The laser was operated in CW mode by turning off the acousto-optic modulator and had a spectral FWHM (full width at half maximum) bandwidth less than 1nm. The beam passes through a converging lens (focal length 40cm) and focused on the surface of the sample after elevated using a periscope mirror configuration. The incidence angle is set to be  $\alpha = 72.4^\circ$ . The refractive index of the diluted Intralipid-10% suspension is  $n = 1.334$  and the extrapolation length is computed to be  $z_e = 1.69l_t$ .<sup>11</sup> Backscattered light in the direction normal to the surface of the sample is recorded by a CCD camera for the wavelengths from 760nm to 860nm with a step of 10nm.

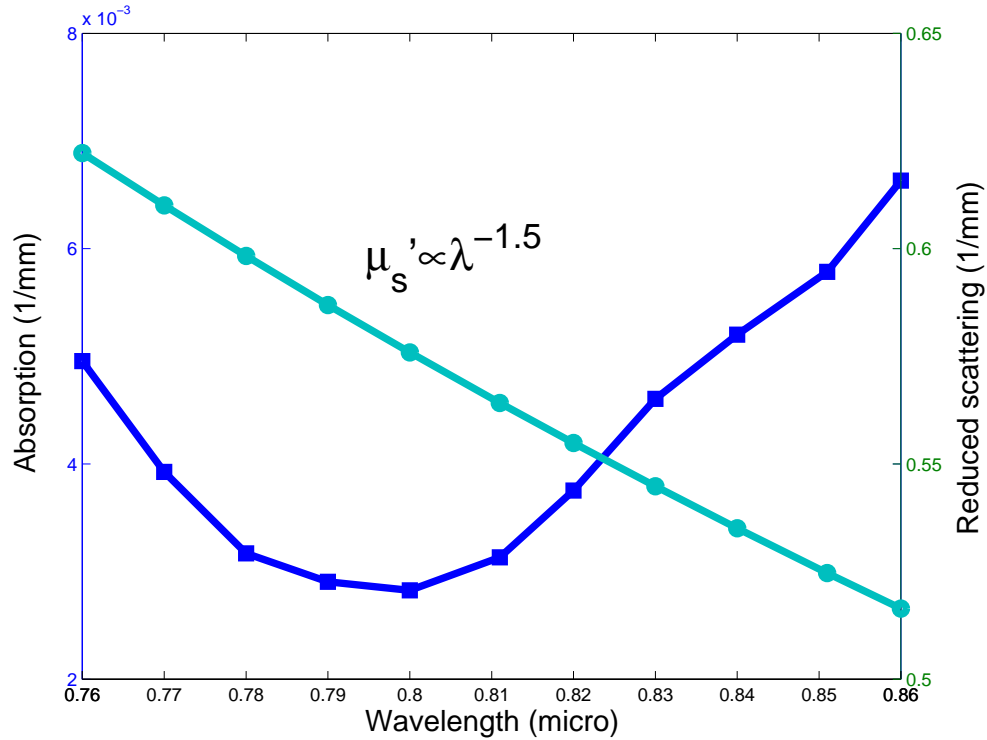


**Figure 3.** The wavelength dependence of the absorption and the reduced scattering coefficients of the Intralipid-10% suspension.

### 3. RESULT

Fig. 3 displays the wavelength dependence of  $\mu_a$  and  $\mu'_s$  from fitting the total diffuse reflectance where light is collected regardless of its polarization. The absorption spectrum follows essentially that of water. The wavelength dependence of the reduced scattering coefficient follows  $\mu'_s \propto \lambda^{-1.5}$ . The fractal dimension of the Intralipid-10% suspension is then 4.5. It should be noted this experimental value of  $D_f$  is a bit larger than the value ( $D_f = 4.2$ ) obtained<sup>2</sup> from the Mie scattering computation based on the particle size distribution of the Intralipid-10% suspension measured by Staveren *et. al.*<sup>12</sup>

The depolarized diffuse reflectance is then measured at the wavelength of 800nm at which the absorption coefficient and the transport mean free path have been found to be  $\mu_a = 0.003\text{mm}^{-1}$  and  $l_t = 1.77\text{mm}$ , respectively, from Fig. (3). Fig. 4 displays the total backscattered light  $I = I_+ + I_-$  and the depolarized backscattered light  $\Delta I = I_+ - I_-$ . Nearby the origin, the intensity of the cross-polarized light is stronger than that of the co-polarized light and  $\Delta I < 0$ . In the far zone (the region far away from the origin), the intensity of the co-polarized light is stronger than that of the cross-polarized light and  $\Delta I > 0$ . Fitting of the depolarized diffuse reflectance  $\propto \Delta I$  along a horizontal line  $3l_t$  away from the incidence point inside the far zone yields the effective absorption  $\mu'_a = 0.47\text{mm}^{-1}$ . The uncoiling length is then 2.13mm and the ratio  $l_x/l_t = 1.20$ .

From the analysis of the depolarization property of the fractal continuous medium of  $D_f = 4.5$  (see Fig. 1), both the g-factor and the cut-off size parameter are now obtained. We find  $g = 0.68$  at the cutoff size parameter 3.4 with  $l_{\text{max}} = 0.32\mu\text{m}$ . The values of the g-factor and the cutoff size of scatterers were reported to be 0.64 at 800nm and  $0.34\mu\text{m}$  in Staveren *et. al.*<sup>12</sup> Their agreement demonstrates the effectiveness of our proposed method.

### 4. DISCUSSION AND CONCLUSION

For a range of values of  $l_x/l_t$  in Fig. 1, there may be two sets of the g-factor and the cutoff size parameter giving the same ratio  $l_x/l_t$ . It does not pose any difficulty. The left branch of the  $l_x/l_t$  curve when the cutoff size parameter curve is less than 2.6 corresponds to  $I_+ < I_-$  and its right branch corresponds to  $I_+ > I_-$  far away from the incidence point.<sup>7</sup> The

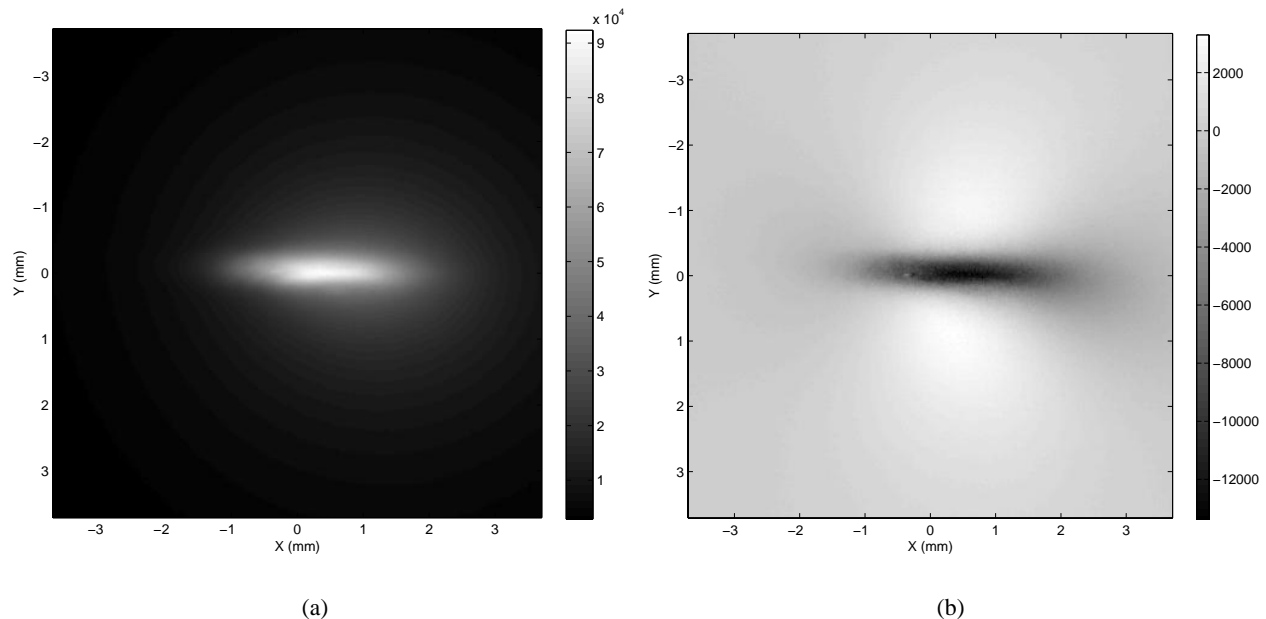


**Figure 4.** The intensities of backscattered light (a) the total intensity  $I_+ + I_-$  and (b) the depolarized intensity  $I_+ - I_-$ . The circularly polarized light is incident on the origin and with an incident angle of  $72.4^\circ$ . The CCD camera measures  $I_\pm$  directly.

experiment shows that  $I_+ > I_-$  in the far zone (see Fig. 4b) and the right branch of the  $l_x/l_t$  curve should be used in our data analysis.

The absorption coefficient, the scattering coefficient and the anisotropy factor of a highly scattering medium are determined using the diffuse reflectance of an obliquely incident circularly polarized light. This approach obtains simply both the anisotropy factor and the cutoff size parameter for the fractal continuous scattering medium from circular depolarization of the backscattered light.

### ACKNOWLEDGMENTS

This work is supported in part by ONR, NASA and USAMRMC grants. MX acknowledges Fairfield University for start-up funds.

### REFERENCES

1. M. Xu and R. R. Alfano, "Fractal mechanisms of light scattering in biological tissue and cells," *Opt. Lett.* **30**, pp. 3051–3053, 2005.
2. M. Xu, M. Alrubaiee, and R. R. Alfano, "Fractal mechanism of light scattering for tissue optical biopsy," in *Optical Biopsy VI, Proceedings of SPIE* **6091**, 2006.
3. N. Joshi, C. Donner, and H. W. Jensen, "Noninvasive measurement of scattering anisotropy in turbid materials by nonnormal incident illumination," *Opt. Lett.* **31**, pp. 936–938, 2006.
4. N. J. McCormick, "Analytic inverse radiative transfer equations for atmospheric and hydrologic optics," *J. Opt. Soc. Am. A* **21**, pp. 1009–1017, June 2004.
5. L. G. Henyey and J. L. Greenstein, "Diffuse radiation in the galaxy," *Astrophys. J.* **93**, pp. 70–83, 1941.
6. M. Xu and R. R. Alfano, "Random walk of polarized light in turbid media," *Phys. Rev. Lett.* **95**, p. 213905, 2005.
7. M. Xu and R. R. Alfano, "Circular polarization memory of light," *Phys. Rev. E* **72**, p. 065601(R), 2005.
8. H. C. van de Hulst, *Light Scattering by Small Particles*, Dover, New York, 1981.
9. M. Xu and R. R. Alfano, "Light depolarization by tissue and phantoms," in *Optical Interactions with Tissue and Cells XVII, Proceedings of SPIE* **6084**, 2006.

10. G. Marquez and L. V. Wang, "White light oblique incidence reflectometer for measuring absorption and reduced scattering spectra of tissue-like turbid media," *Opt. Express* **1**, pp. 454–460, 1997.
11. J. X. Zhu, D. J. Pine, and D. A. Weitz, "Internal reflection of diffusive light in random media," *Phys. Rev. A* **44**, pp. 3948–3959, 1991.
12. H. J. van Staveren, C. J. M. Moes, J. van Marle, S. A. Prahl, and M. J. C. van Gemert, "Light scattering in Intralipid-10% in the wavelength range of 400-1100nm," *Appl. Opt.* **30**(31), pp. 4507–4514, 1991.